

# Modelling Nanoparticles Distribution Pattern in a Microchannel Flow of Nano Fluid Filled with a Porous Medium

*O. D. Makinde\* and R. L. Monaledi*

Faculty of Military Science, Stellenbosch University, Private Bag X2, Saldanha 7395, South Africa.

Received: 3 May. 2019, Revised: 2 Jul. 2019, Accepted: 2 Sep. 2019.

Published online: 1 Nov. 2019.

**Abstract:** In this paper, a modified Buongiorno model is proposed and utilized to examine the nanoparticles distribution pattern in a nanofluid flow through a microchannel filled with a porous medium. The governing nonlinear differential equations are obtained and tackled numerically by using shooting method coupled with Runge-Kutta-Fehlberg integration scheme. Graphical results showing the effects of the pertinent parameters on the nanofluid velocity, nanoparticles concentration, skin friction and Sherwood number are presented and discussed quantitatively. It is found that nanoparticles tend to aggregate with high concentration along the microchannel centreline region, thus, lessens the skin friction and boosts the Sherwood number.

**Keywords:** Nanofluid; Microchannel; Poiseuille Flow; Nanoparticles Distribution; Porous Medium.

## Nomenclature

$u$	Velocity components ( $\text{ms}^{-1}$ )	<b>Greek symbols</b>	
$(x,y)$	Coordinates (m)	$\eta$	Dimensionless variable
$C$	Nanoparticles concentration	$\mu_f$	Base fluid dynamic viscosity( $\text{kgm}^{-1}\text{s}^{-1}$ )
$C_w$	Wall concentration	$\mu_{nf}$	Nanofluid dynamic viscosity( $\text{kgm}^{-1}\text{s}^{-1}$ )
$C_s$	Total nanoparticles concentration	$\nu_f$	Nanofluid kinematic viscosity( $\text{m}^2\text{s}^{-1}$ )
$K$	Permeability	$\rho_f$	Density ( $\text{kgm}^{-3}$ )
$h$	Microchannel width (m)	$\tau_w$	Wall shear stress (Pa)
$L$	Microchannel length (m)		
$Sh$	Sherwood number		
$Re$	Reynolds number		
$Da$	Darcy number		
$q_m$	Mass flux ( $\text{Wm}^{-2}$ )		
$W$	Dimensionless velocity		

## 1 Introduction

Microfluidics has become an emerging science and technology of systems that process nano-sized fluid materials using channels with dimensions of tens to hundreds of micrometres [1-3]. Adequate knowledge of fluid flows in microchannels are crucial for the effective control of dynamic effects associated with transport phenomena such as momentum, heat and mass transfer for different applications in micro-system technology. Moreover, the enormously small aspect ratio characteristics of microchannels offer a veritable platform for enhance flow rate with heat and mass transfer processes such as the transportation of fluids for chemical or biological processing, micro-mixing of different fluids or separating different species and micro-scaled cooling systems of electronic devices [4, 5]. Meanwhile, it is reported that the surface contact area to-volume ratio of the flow is enhanced by incorporating porous media into the microchannels [6, 7]. Consequently, the embedment of porous media in microchannels will further improve the local velocity mixing of working fluid and provide a high-mass-flux removal method in miniaturized devices.

Recently, the advancement in the field of nanotechnology have led to the advent of a new generation of coolants known as nanofluids [8, 9]. It is engineered by colloidal suspensions of functionalized nano-sized particles composite materials into the

\*Corresponding author e-mail: [makinded@gmail.com](mailto:makinded@gmail.com)

based fluid. Some typical nanofluids are ethylene glycol based copper or silver nanofluids and water based copper oxide or iron oxide nanofluids [10, 11]. In spite of the existence of numerous experimental and theoretical investigations [12-15] on micro-porous channel hydrodynamics of nanofluids, a number of principal problems are not well studied especially with respect to the impact of nanoparticles distribution pattern on flow rate and mass flux. In the present studies, the objective is to fill this gap by theoretically examining the combined effects of porous medium permeability and nanoparticles distribution pattern on both flow rate and mass transfer rate in a micro-porous channel. In the following sections, the model problem is formulated, analyzed and numerically tackled. Pertinent results for the velocity and nanoparticles concentration profiles as well as the skin friction and Sherwood number are obtained. Effects of various physical parameters are displayed graphically and discussed.

## 2 Model Problems

The modified Buongiorno [9] model for a Poiseuille flow of an incompressible nanofluid with variable viscosity in a microchannel filled with a porous medium is considered as shown in figure 1. The flow takes place in the  $x$  - direction between two parallel plates of small width  $h$  and very long length  $L$ . Following [16], the nanoparticle concentration dependent nanofluid dynamic viscosity ( $\mu_{nf}$ ) can be expressed as

$$\mu_{nf} = \frac{\mu_f (C_s - C_w)^{2.5}}{(C_s - C)^{2.5}}, \quad (1)$$

Where  $C_s$  is the total concentration of nanoparticles such that  $C_w < C \ll C_s$ ,  $\mu_f$  is the base fluid dynamic viscosity,  $C_w$  is the nanoparticles concentration at the microchannel walls and  $C$  is the nanofluid concentration.

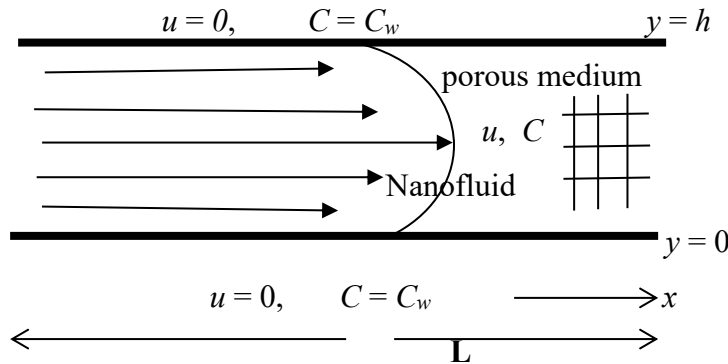


Fig. 1: Schematic diagram of the problem.

Under these conditions, the continuity, momentum and nanoparticles concentration equations governing the problem may be written as [11, 13-15];

$$\frac{\partial u}{\partial x} = 0, \quad (2)$$

$$\frac{\partial}{\partial y} \left( \mu_{nf} \frac{\partial u}{\partial y} \right) - \frac{\mu_{nf} u}{K} - \frac{\partial P}{\partial x} = 0, \quad (3)$$

$$D_B \frac{\partial^2 C}{\partial y^2} + \gamma (C_s - C) = 0, \quad (4)$$

with the boundary conditions given as

$$\left. \begin{aligned} u = 0, \quad T = T_w, \quad C = C_w, \quad \text{at } y = 0 \\ u = 0, \quad T = T_w, \quad C = C_w, \quad \text{at } y = h \end{aligned} \right\} \quad (5)$$

where  $D_B$  is the nanoparticles mass diffusivity,  $\rho_f$  is the base fluid density,  $P$  is the nanofluid pressure,  $\gamma$  relates to the source rate of nanoparticles into the nanofluid. We introduce the following non-dimensional quantities in equations (2) - (5):

$$\eta = \frac{y}{h}, W = \frac{uh}{\nu_f}, \phi = \frac{C - C_w}{C_s - C_w}, \nu_f = \frac{\mu_f}{\rho_f}, \lambda = \frac{\gamma h^2}{\nu_f},$$

$$A = -\frac{\partial \bar{P}}{\partial X}, \bar{P} = \frac{\rho_f h^2 P}{\mu_f^2}, X = \frac{x}{h}, Sc = \frac{\nu_f}{D_B}, Da = \frac{K}{h^2},$$

and obtain

$$\frac{d^2 W}{d\eta^2} + \frac{5}{2(1-\phi)} \frac{dW}{d\eta} \frac{d\phi}{d\eta} - \frac{W}{Da} + A(1-\phi)^{\frac{5}{2}} = 0, \tag{7}$$

$$\frac{d^2 \phi}{d\eta^2} + Sc\lambda(1-\phi) = 0, \tag{8}$$

with boundary conditions given as

$$\left. \begin{aligned} W(0) = \phi(0) = 0, \\ W(1) = \phi(1) = 0, \end{aligned} \right\} \tag{9}$$

where A corresponds to the constant axial pressure gradient, Sc is the Schmidt number, Da is the Darcy number and  $\lambda$  is the parameter that relates to the rate of injection of nanoparticles into the base fluid. Other quantities of interest are the skin friction coefficients ( $C_f$ ) and the Sherwood number ( $Sh$ ) which are given as

$$C_f = \frac{h^2 \tau_w}{\rho_f \nu_f^2} = \frac{dW}{d\eta} \Big|_{\eta=0,1}, \quad Sh = \frac{hq_m}{D_B(C_1 - C_w)} = -\frac{d\phi}{d\eta} \Big|_{\eta=0,1}, \tag{10}$$

where

$$\tau_w = \mu_{nf} \frac{\partial u}{\partial y}, \quad q_m = -D_B \frac{\partial C}{\partial y}. \tag{11}$$

### 3 Numerical Procedures

The nonlinear model boundary value problem in equations (7)-(9) are transformed into a set of first order ordinary differential equations with some unknown initial conditions and tackled numerically using shooting method with Runge-Kutta-Fehlberg integration scheme [17].

Let  $W = y_1, W' = y_2, \phi = y_3, \phi' = y_4.$  (12)

The governing equations then become

$$\left. \begin{aligned} y_1' &= y_2 \\ y_2' &= -\frac{5y_2 y_4}{2(1-y_3)} + \frac{y_1}{Da} - A(1-y_3)^{\frac{5}{2}} \\ y_3' &= y_4 \\ y_4' &= Sc\lambda(y_3 - 1) \end{aligned} \right\} \tag{13}$$

with the corresponding initial conditions as

$$y_1(0) = 0, y_2(0) = a_1, y_3(0) = 0, y_4(0) = a_2. \tag{14}$$

The values of  $a_1$  and  $a_2$  in the equation (14) are initially guessed and thereafter accurately determined via shooting method with Newton-Raphson's iteration technique for each set of parameter values in equation (13) with step size of  $\Delta\eta=0.01$ . Solutions obtained for the velocity and nanoparticles concentration profiles are utilized to compute the values for the skin friction and Sherwood number as given in equation (10).

### 4 Results and Discussion

In order to gain an insight into the overall flow structure with mass transfer characteristics, numerical solution for the velocity and nanoparticles concentration profiles are presented graphically in figures 2-6. We also compute the results for the skin friction ( $C_f$ ) and Sherwood number ( $Sh$ ) as depicted in figures 7-9. Generally, the velocity profiles as illustrated in figures 2-4 are parabolic with maximum value along the microchannel centreline region and zero at the walls due to no slip condition. It is noteworthy that an increase in the Darcy number (Da) enhances the nanofluid velocity due to an enlarge

Permeability of the porous media (see figure 2). Meanwhile, the velocity profiles lessens with a rise in the parameter values of  $Sc$  and  $\lambda$ . This can be attributed to the thickening of the nanofluid due to increasing concentration of nanoparticles, consequently, the nanofluid viscosity rises and the flow rate diminishes as depicted in figures 3-4.

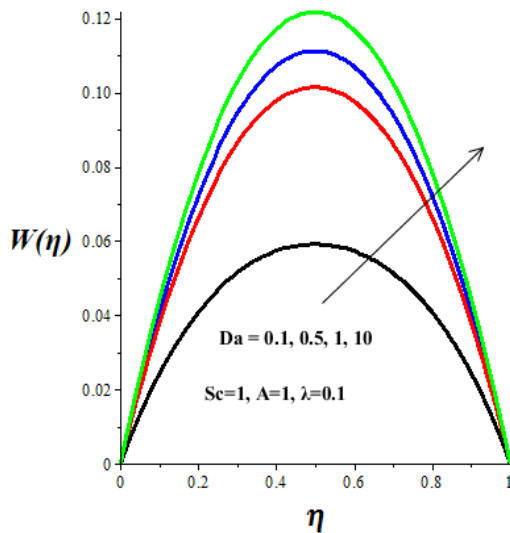


**Fig. 2:** Effect of  $Da$  on velocity profiles.

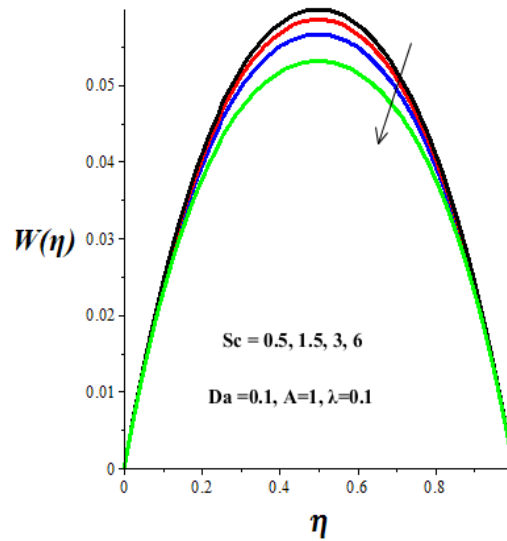


**Fig. 3:** Effect of  $Sc$  on velocity profiles.

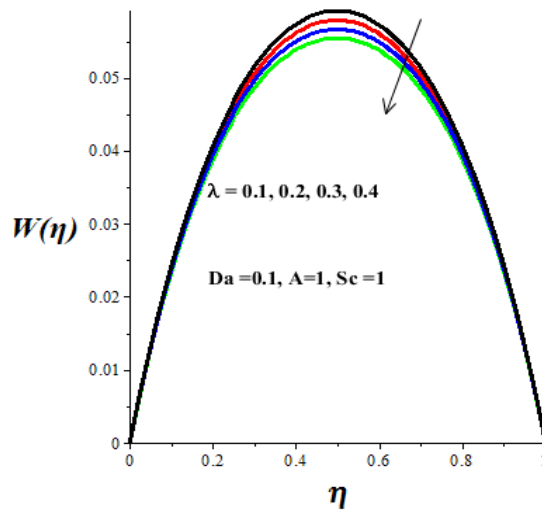


**Fig. 4:** Effect of  $\lambda$  on velocity profiles.

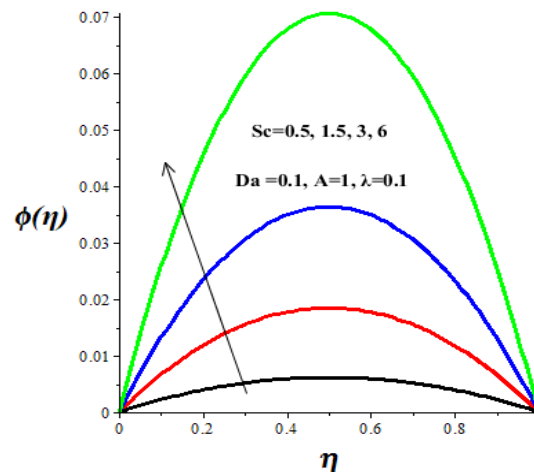


**Fig. 5:** Nanoparticles concentration profiles with  $Sc$ .

In figures 5-6, we observed that nanoparticles tend to aggregate more towards the microchannel centreline region with high concentration as compare to the wall region. Moreover, this distribution pattern of nanoparticles is enhanced with an amplification in the parameter values of  $Sc$  and  $\lambda$ . This is expected, since an increase in the values  $Sc$  and  $\lambda$  implies more injection of nanoparticles into the base fluid, leading to a rise in the concentration of nanoparticles towards the microchannel centreline region.

Figures 7-8 show that the shear stress (skin friction) at the microchannel wall lessens with a rise in parameter values of  $Sc$  and  $\lambda$ , but escalates with an increase in parameter values of  $A$  and  $Da$ . Since the nanofluid viscosity is augmented with increasing values of  $Sc$  and  $\lambda$ , consequently, velocity gradient at the wall diminished, leading to a fall in skin friction. Meanwhile, as  $A$  and  $Da$  values increase, the velocity gradient at the wall is enhanced, leading to skin friction amplification. In figure 9, it is seen that nanoparticles mass transfer rate at the wall increases with both  $Sc$  and  $\lambda$ . This is expected since the

injection of nanoparticles into the base fluid rises with increase values of  $Sc$  and  $\lambda$ , leading to a boost in the nanoparticles concentration gradient at the wall and enhanced Sherwood number.

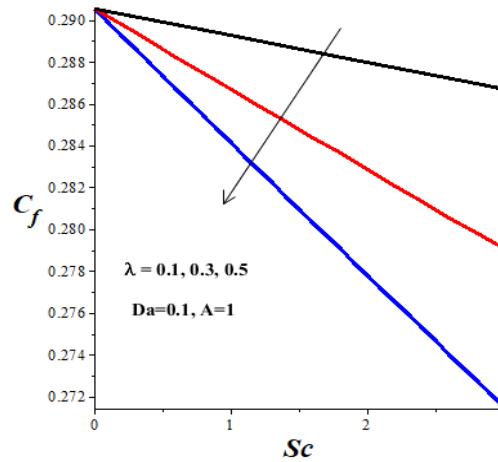
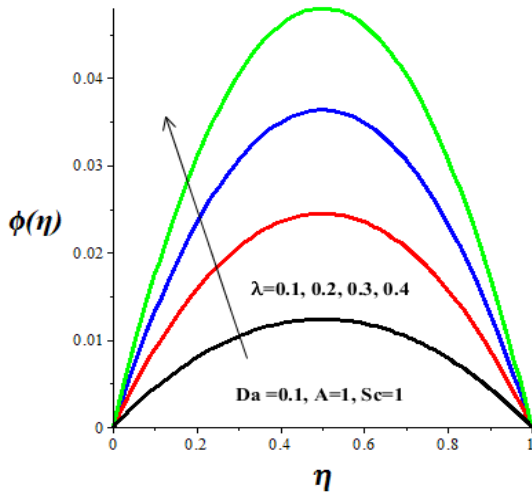


**Fig. 6:** Nanoparticles concentration profiles with  $\lambda$ .

**Fig. 7:** Skin friction with  $Sc$  and  $\lambda$ .

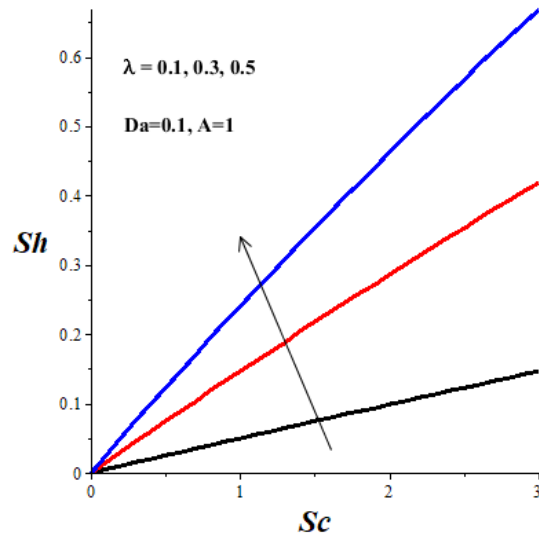
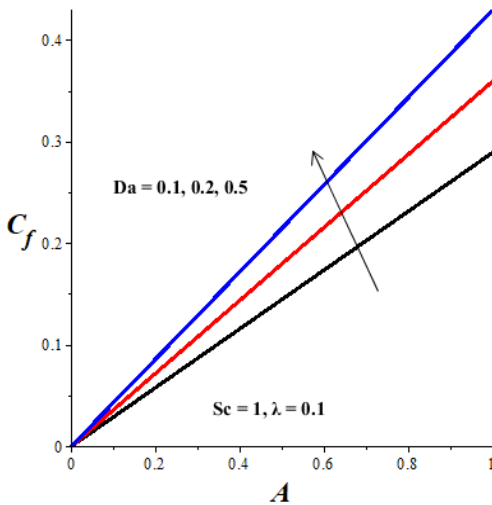


**Fig. 8:** Skin friction with  $A$  and  $Da$ .

**Fig. 9:** Sherwood number with  $Sc$  and  $\lambda$ .

### 5 Conclusions

In this study, variable viscosity nanofluid Poiseuille flow in a microchannel filled with a porous medium has been investigated numerically using shooting method coupled with Runge-Kutta-Fehlberg integration scheme. Pertinent results can be summarized as follows:

- Increase in  $Sc$  and  $\lambda$  lessen the velocity profiles but enhance the nanoparticles concentration profiles.
- Increase in  $Da$  boosts the velocity profiles.
- Nanoparticles tend to aggregate more towards the microchannel centreline region as compare to the wall region
- Skin friction diminishes with a rise in  $Sc$  and  $\lambda$ , but amplifies with an increase in  $A$  and  $Da$ .
- Increase in  $Sc$  and  $\lambda$  boost the Sherwood number.

Finally, it is worth mentioning that the observed distribution pattern of nanoparticles with high concentration along the microchannel centreline region augments the efficient flow process through the reduction of the skin friction and enhancement of the Sherwood number.

## References

- [1] C. Richter, F. Kotz, N. Keller, T. M.Nargang, K. Sachsenheimer, D. Helmer, B.E. Rapp, An analytical solution to neumann-type mixed boundary poiseuille microfluidic flow in rectangular channel cross-sections (slip/no-slip) including a numerical technique to derive it. *Journal of Biomedical Science and Engineering.*, **10**, 205-219, 2017.
- [2] Y. Li, W. Van Roy, L. Lagae, P.M. Vereecken, Analysis of fully on-chip microfluidic electrochemical systems under laminar flow. *Electrochimica Acta.*, **231**, 200-208, 2017
- [3] T. M. Squires, S.R. Quake, Microfluidics: Fluid physics at the nanoliter scale. *Rev Mod Phys.*, **77**, 977-1026, 2005.
- [4] N.T. Obot, Toward a better understanding of friction and heat/mass transfer in microchannel – A literatures review, *Microscale Thermophysical Engineering.*, **6**, 155-173, 2002.
- [5] C. Yang, D. Li, J.H. Masliyah, Modeling forced liquid convection in rectangular microchannels with electrokinetic effects, *International Journal of Heat and Mass Transfer.*, **41**, 4229-4249, 1998.
- [6] P.X. Jiang, M.H. Fan, G.S. Si, Z.P. Ren, Thermal-hydraulic performance of small scale micro-channel and porous-media heat-exchangers, *Int. J. Heat Mass Transfer.*, **44**, 1039-1051, 2001.
- [7] T. C. Hung, Y.X. Huang, W.M. Yan, Thermal performance analysis of porous microchannel heat sinks with different configuration designs, *Int. J. Heat Mass Transfer.*, **66**, 235-243, 2013.
- [8] S.U.S. Choi, Enhancing thermal conductivity of fluids with nanoparticles in development and applications of non-Newtonian flows, *ASME New York.*, 99-103, 1995.
- [9] J. Buongiorno, Convective transport in nanofluids, *ASME J. Heat Transf.*, **128**, 240-250, 2006.
- [10] S. Das, R.N. Jana, O.D. Makinde, MHD flow of Cu-Al<sub>2</sub>O<sub>3</sub>/Water hybrid nanofluid in porous channel: Analysis of entropy generation, *Defect and Diffusion Forum.*, **377**, 42-61, 2017.
- [11] R.L. Monaedi, O.D. Makinde, Entropy analysis of a radiating variable viscosity EG/Ag nanofluid flow in microchannels with buoyancy force and convective cooling, *Defect and Diffusion Forum.*, **387**, 273-285, 2018.
- [12] J. M. Koo, C. Kleinstreuer, Liquid flow in microchannels: Experimental observations and computational analyses of microfluidics effects. *J Micromech Microeng.*, **13**, 568-579, 2003.
- [13] O.D. Makinde, A.S. Eegunjobi, MHD couple stress nanofluid flow in a permeable wall channel with entropy generation and nonlinear radiative heat, *Journal of Thermal Science and Technology.*, **12(2)**, 17-00252-JTST0033(16pages), 2017.
- [14] M. Venkateswarlu, M. Prameela, O.D. Makinde, Influence of heat generation and viscous dissipation on hydromagnetic fully developed natural convection flow in a vertical micro-channel. *Journal of Nanofluids.*, **8(7)**, 1506-1516, 2019.
- [15] M. Venkateswarlu, O.D. Makinde, D.V. Lakshmi, Influence of thermal radiation and heat generation on steady hydromagnetic flow in a vertical micro-porous-channel in presence of suction/injection, *Journal of Nanofluids.*, **8(5)**, 1010-1019, 2019.
- [16] H.C. Brinkman, The viscosity of concentrated suspensions and solutions, *J. Chem. Phys.*, **20**, 571, 1952.
- [17] T. Cebeci, P. Bradshaw, Physical and computational aspects of convective heat transfer, Springer, New York, USA, 1988.